Controllable Goos-Hänchen shifts and spin beam splitter for ballistic electrons in a parabolic quantum well under a uniform magnetic field

Xi Chen,[1,2,*] Xiao-Jing Lu,[1] Yan Wang,[1] and Chun-Fang Li[1,3]

[1]*Department of Physics, Shanghai University, 200444 Shanghai, China*

[2]*Departamento de Química-Física, UPV-EHU, Apdo 644, E-48080 Bilbao, Spain*

[3]*State Key Laboratory of Transient Optics and Photonics, Xi'an Institute of Optics and Precision Mechanics of CAS, 710119 Xi'an, China*

(Received 8 December 2010; revised manuscript received 24 March 2011; published 4 May 2011)

The quantum Goos-Hänchen shift for ballistic electrons is investigated in a parabolic potential well under a uniform vertical magnetic field. It is found that the Goos-Hänchen shift can be negative as well as positive, and becomes zero at transmission resonances. The beam shift depends not only on the incident energy and incidence angle, but also on the magnetic field and Landau quantum number. Based on these phenomena, we propose an alternative way to realize the spin beam splitter in the proposed spintronic device, which can completely separate spin-up and spin-down electron beams by negative and positive Goos-Hänchen shifts.

DOI: 10.1103/PhysRevB.83.195409 PACS number(s): 72.25.Dc, 42.25.Gy, 73.21.Fg, 73.23.Ad

I. INTRODUCTION

The longitudinal Goos-Hänchen shift is well known for a light beam totally reflected from an interface between two dielectric media.[1] This phenomenon, suggested by Sir Isaac Newton, was observed first in a microwave experiment by Goos and Hänchen[2] and theoretically explained by Artmann in terms of a stationary phase method.[3] Up till now, the investigations of the Goos-Hänchen shift have been extended to different areas of physics,[1] such as quantum mechanics,[4,5] acoustics,[6] neutron physics,[7,8] spintronics,[9] atom optics,[10] and graphene,[11–13] based on the particle-wave duality in quantum mechanics.

Historically, the quantum Goos-Hänchen shifts and relevant transverse Imbert-Fedorov shifts were studied for relativistic Dirac electrons in the 1970's.[14,15] With the development of semiconductor technology, the Goos-Hänchen shift for ballistic electrons in two-dimensional electron gas (2DEG) systems became one of the important subjects in the study of ballistic electron wave optics.[16–19] It was found that the lateral shifts of ballistic electrons transmitted through a semiconductor quantum barrier or well can be enhanced by transmission resonances, and the lateral shifts can become negative as well as positive.[19] The interesting Goos-Hänchen shift, depending on the spin polarization, could also provide an alternative way to realize the spin filter and spin beam splitter in spintronics[9] in the same way as other optical-like phenomena, including double refraction[20] and negative refraction[21] in spintronics optics.[22]

In this paper, we will investigate the Goos-Hänchen shifts for ballistic electrons in a parabolic quantum well under a uniform magnetic field, in which the high spin polarization and electron transmission probability can be achieved.[23] It is shown that the lateral shift can be negative as well as positive. As a matter of fact, the Goos-Hänchen shift discussed here is different from that in a magnetic-electric nanostructure,[9] where the δ magnetic field is considered. In such a quantum well, the uniform magnetic field continuously bends the trajectory of the electron, so that the electrons exhibit cyclotron motion. Then this implies that the behavior of electrons in such a system has no direct analogy with the linear propagation of light.[13] Meanwhile, it is also suggested that the Landau quantum number will have a great effect on the Goos-Hänchen shift. We consider the Goos-Hänchen shift for ballistic electrons in a parabolic quantum well under a uniform magnetic field and its dependence on the magnetic field and Landau energy level, which, to the best of our knowledge, has not been investigated so far. More importantly, the Goos-Hänchen shift for ballistic electrons depends on the spin polarization by Zeeman interaction, which is similar to that for neutrons.[8] The realization of the negative and positive Goos-Hänchen shifts corresponding to spin-up and spin-down polarized electrons may have future applications in proposed spintronic devices, such as spin filters and spin beam splitters.

II. THEORETICAL MODEL

We consider a 2DEG structure, with a confining potential in the central region, as shown in Fig. 1(a). The confinement potential is assumed to be parabolic in the transverse y direction, and the electron transports in the 2DEG occur in the x-y plane. A uniform magnetic B field is applied along the perpendicular z direction and limited to within the parabolic confinement region. In practice, such a B-field configuration can be achieved by means of a ferromagnetic gate stripe on top of the 2DEG heterostructure.[23] The Hamiltonian within the parabolic quantum well is then given by

$$H = (1/2m)(\mathbf{p} - \mathbf{A})^2 + H_{\text{conf}} + H_z, \tag{1}$$

where m is the effective mass of the electron and $\mathbf{p}$ is the momentum of the electron. The Landau gauge is chosen for the magnetic vector potential, i.e., $\mathbf{A} = (By,0,0)$, where B is the magnetic field strength. The parabolic confinement energy can be expressed as $H_{\text{conf}} = \frac{1}{2}m\omega_0^2 y^2$, while the Zeeman interaction term is given by $H_z = \frac{1}{2}\mu_B g\sigma B$, so μ_B is the Bohr magneton, g is the Landé factor, and $\sigma = \pm 1$ denotes the spin orientation parallel or antiparallel to the reference z axis. In this system, the wave functions of a plane wave for electrons in three regions can be expressed as

$$\Psi_{\text{I}}(x,y) = (e^{ik_x x} + Ae^{-ik_x x})e^{ik_y y}, \quad x < 0, \tag{2}$$

$$\Psi_{\text{II}}(x,y) = (Be^{ik'_x x} + Ce^{-ik'_x x})\psi_2(y), \quad 0 < x < d, \tag{3}$$

$$\Psi_{\text{III}}(x,y) = De^{ik_x(x-d)}e^{ik_y y}, \quad x > d, \tag{4}$$

where $k_x = \sqrt{2mE/\hbar^2 - k_y^2}$ is the traveling wave vector in 2DEG. The Schrödinger equation in the parabolic potential region can be written in the form of a harmonic oscillator centered at $\widetilde{Y}$ with angular frequency $\widetilde{\omega}_c$,

$$\left[\frac{m\widetilde{\omega}_c^2}{2}(y-\widetilde{Y})^2+\frac{m\omega_0^2\omega_c^2}{2\widetilde{\omega}_c^2}Y^2+\frac{\mu_B g\sigma}{2}B-\frac{\hbar^2}{2m}\frac{d^2}{dy^2}\right]\Psi_{\rm II}=E\Psi_{\rm II}, \tag{5}$$

with $\widetilde{Y} = (\omega_c/\widetilde{\omega}_c)^2 Y$, $\widetilde{\omega}_c^2 = \omega_0^2 + \omega_c^2$, $\omega_c = eB/m$, $Y = \hbar k_x'/eB$, and ω_c is the cyclotron frequency. So the solution is given by a linear combination of Hermite polynomials as follows:

$$\psi_2(y) = \left(\frac{1}{2^n n!\gamma\sqrt{\pi}}\right)^{1/2} e^{-[(y-\widetilde{Y})^2/2\gamma^2]} H_n\left(\frac{y-\widetilde{Y}}{\gamma}\right), \tag{6}$$

where $\gamma^2 = \hbar/\sqrt{e^2B^2+m^2\omega_0^2}$. The corresponding eigenenergy is

$$E_n = \left(n+\frac{1}{2}\right)\hbar\widetilde{\omega}_c + \frac{m\omega_0^2\omega_c^2}{2\widetilde{\omega}_c^2}Y^2 + \frac{1}{2}\mu_B g\sigma B. \tag{7}$$

The eigenstates of the system form a set of Landau-like states with energy splitting proportional to B. Within the central potential region, the longitudinal wave vector k_x' is given by

$$k_x' = \sqrt{\frac{2m\widetilde{\omega}_c^2[E_n - (n+\frac{1}{2})\hbar\widetilde{\omega}_c - \frac{1}{2}\mu_B g\sigma B]}{\hbar^2\omega_0^2}}, \tag{8}$$

which is spin dependent due to the Zeeman interaction. Interestingly, when only the plane wave is considered, the spatial location of the eigenstates inside the region of the potential well is around $Y = \hbar k_x'/eB$, which can be rewritten by

$$Y = v(n,k_x')\frac{\omega_0^2+\omega_c^2}{\omega_c\omega_0^2}, \tag{9}$$

with a velocity

$$v(n,k_x') = \frac{1}{\hbar}\frac{\partial E_n}{\partial k_x'} = \frac{\omega_0^2}{\widetilde{\omega}_c^2}\frac{\hbar k_x'}{m}. \tag{10}$$

The transverse location for each plane-wave eigenstate is proportional to the velocity and magnetic field. From a classical viewpoint, the spatial shift can be reasonably explained by the Lorentz force.[24] As a consequence, the transverse shifts for the forward and backward propagating states inside the central region are positive and negative, since the Lorentz force is opposite for electrons moving in the opposite direction. However, the lateral shift predicted by the Goos-Hänchen effects will be completely different. In what follows, we will discuss the spin-dependent Goos-Hänchen shift of electron beams, instead of the plane wave, in such a configuration.

III. GOOS-HÄNCHEN SHIFTS AND SPIN BEAM SPLITTER

A. Stationary phase method

When the finite-sized incident electron beam is considered, the wave function of the incident beam can be assumed to be

$$\Psi_{\rm in}(x,y) = \frac{1}{\sqrt{2\pi}}\int A(k_y - k_{y0})e^{i(k_x x + k_y y)}\,dk_y, \tag{11}$$

with the angular spectrum distribution $A(k_y - k_{y0})$ around the central wave vector k_{y0}, then the transmitted beam can be expressed by

$$\Psi_{\rm tr}(x,y) = \frac{1}{\sqrt{2\pi}}\int DA(k_y - k_{y0})e^{i[k_x(x-d)+k_y y]}\,dk_y, \tag{12}$$

where the transmission coefficient $D = \exp(i\phi)/g$ is determined by the boundary conditions at $x = 0$ and $x = d$ with

$$g\exp(i\phi) = \cos(k_x' d) + i\left(\frac{k_x^2 + k_x'^2}{2k_x k_x'}\right)\sin(k_x' d), \tag{13}$$

which leads to the phase shift ϕ in terms of

$$\tan\phi = \frac{k_x^2 + k_x'^2}{2k_x k_x'}\tan(k_x' d). \tag{14}$$

To find the position where $\Psi_{\rm tr}(x,y)$ is maximum, that is, the lateral shift of the transmitted beam, we look for the place where the phase of the transmitted beam, $\Phi = k_x(x-d) + k_y y + \phi$, has an extremum when differentiated with respect to k_y, i.e., $\partial\Phi/\partial k_y = 0$.[25] So, according to the stationary phase approximation, the Goos-Hänchen shift for ballistic electrons at $x = d$ is defined as[9]

$$s = -\frac{d\phi}{dk_{y0}}. \tag{15}$$

It is noted that the subscript 0 denotes the value at $k_y = k_{y0}$, namely, $\theta = \theta_0$. Thus, the Goos-Hänchen shift, as described in Fig. 1(b), can be obtained by

$$s = \frac{d\tan\theta_0}{2g_0^2}\left(1 - \frac{k_{x0}'^2}{k_{x0}^2}\right)\frac{\sin(2k_{x0}' d)}{2k_{x0}' d}, \tag{16}$$

where θ_0 is the incidence angle and $\tan\theta_0 = k_{y0}/k_{x0}$. Obviously, it is clearly seen from Eq. (16) that the Goos-Hänchen shifts are negative as well as positive, depending on $k_{x0}'^2/k_{x0}^2$ and $\sin(2k_{x0}' d)$.

In the propagating case, when the transmission resonances $k_{x0}' d = m\pi$ $(m = 1,2,3,\ldots)$ or antiresonances $k_{x0}' d = (m + 1/2)\pi$ $(m = 1,2,3,\ldots)$ occur, the Goos-Hänchen shift is zero, which means the positions in the y direction are the same for both incident and transmitted electrons. As a matter of fact, when measured with reference to the geometrical prediction from electron optics, the "zero" lateral shifts will become

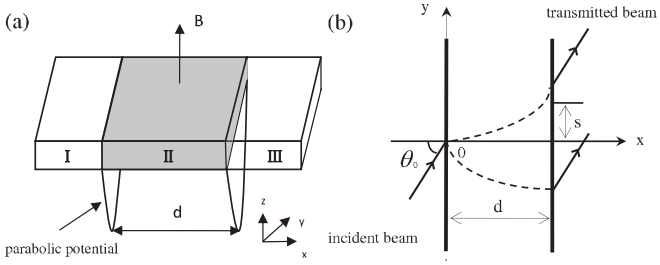

FIG. 1. (a) Schematic diagram for a 2DEG with a parabolic quantum well under a uniform magnetic field. (b) Negative and positive Goos-Hänchen shifts of ballistic electrons are presented in this configuration.

essentially negative values, whereas when the incident energy is less than the critical energy,

$$E < E_c = \left(n + \tfrac{1}{2}\right)\hbar\widetilde{w}_c + \tfrac{1}{2}\mu_B g\sigma B, \tag{17}$$

k'_{x0} becomes imaginary, thereby $k'^2_{x0}/k^2_{x0} < 0$. Substituting $k'_{x0} = i\kappa_0$ into Eq. (16), we end up with the following expression:

$$s = \frac{d\tan\theta_0}{2g'^2_0}\left(1 + \frac{\kappa_0^2}{k_{x0}^2}\right)\frac{\sinh(2\kappa_0 d)}{2\kappa_0 d}, \tag{18}$$

with

$$g'^2_0 = \cosh^2(\kappa_0 d) + \left(\frac{k_x^2 - \kappa_0^2}{2k_x\kappa_0}\right)^2 \sinh^2(\kappa_0 d). \tag{19}$$

In the evanescent case, the Goos-Hänchen shifts are always positive, which seems similar to the Goos-Hänchen shifts in a single semiconductor barrier.[18] In the opaque limit, $\kappa_0 d \gg 1$, the lateral shift saturates to

$$s = \frac{2\kappa_0\tan\theta_0}{k_{x0}^2 + \kappa_0^2} \simeq \frac{2\tan\theta_0}{\kappa_0}, \tag{20}$$

which is independent of the width d of the potential well. In the following discussions, we will study the Goos-Hänchen shifts for different polarized electrons and their modulation by the magnetic field.

First of all, an example of the Goos-Hänchen shifts (in units of $\lambda_e = 2\pi\hbar/\sqrt{2m_e E}$) for ballistic electrons as functions of incident energy E/E_0 in the quantum well under a uniform vertical magnetic field is displayed in Fig. 2(a), where the quantum well is made from an InSb semiconductor, the physical parameters are, respectively, $m = 0.013m_e$, m_e is the bare electron mass, $g = 51$, the length of potential well is $d = 50$ nm, with a parabolic well of depth $\hbar\omega_0 = 2$ meV, an applied magnetic field of $B = 0.5$ T, $n = 5$, and $E_0 = \hbar\omega_c = 4.45$ meV. It is clearly seen from condition (17) that the critical energies are different for spin-up and spin-down polarized electrons, which correspond to $E_c^+ = 26.11$ meV and $E_c^- = 27.58$ meV, respectively, for the parameters used here. As shown in Fig. 2 (a), the behavior of the Goos-Hänchen shifts coincides with the theoretical analysis mentioned above, that is to say, the Goos-Hänchen shifts are always positive when the incident energy is less than the critical energy E_c, while the lateral shifts become negative as well as positive periodically as related to the transmission resonances. In addition, Fig. 2(b) also shows the dependence of transmission probability $T = |D|^2$ on the incident energy. This quantity can be connected with the measurable ballistic conductance G, according to the well-known Landauer-Büttiker formula at zero or nonzero temperature.[24,26]

More interestingly, the spin-up and spin-down polarized electron beams can be separated by spatial shifts, due to their energy dispersion relation depending on the polarization. Based on the properties of the Goos-Hänchen shifts, the simplest way to realize the energy filter by the Goos-Hänchen shifts is as follows. We can choose the incident energy within the range of $E_c^+ < E < E_c^-$. This suggests that the spin-down polarized electrons for $E > E_c^-$ can traverse through the structure in a propagating mode with a high transmission probability, while the spin-up polarized electrons for $E < E_c^+$ tunnel through it in the evanescent mode with a very low transmission probability, as described in Fig. 2(b). So this provides an alternative way to design a spin spatial filter with an energy width $\Delta E = \mu_B g B = 1.46$ meV for the parameters in Fig. 2.

Next, we will discuss the influence of magnetic field and Landau energy level on the Goos-Hänchen shifts in such a semiconductor device. Figure 3 illustrates the dependence of the Goos-Hänchen shifts on the strength of magnetic field B with different Landau quantum numbers n, where $n = 0$ (a), $n = 1$ (b), $n = 3$ (c), $n = 5$ (d), $\theta_0 = 70^\circ$, $E = 17.81$ meV, and the other physical parameters are the same as those in Fig. 2. Solid (red) and dashed (blue) lines correspond to spin-up and spin-down polarized electrons. Basically, the behavior of the Goos-Hänchen shifts is different from that of transverse shifts for the plane wave, as described in Sec. II. According to the definition of critical energy E_c, under the low strength of magnetic field, the incident energy will be larger than the critical energy, thus the electron can propagate though the quantum well with negative and positive Goos-Hänchen shifts, which can be adjusted by the conditions

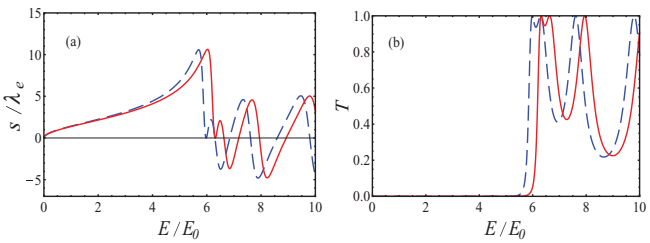

FIG. 2. (Color online) Dependence of the Goos-Hänchen shift (a) and transmission probability (b) on the incident energy E/E_0, where $\theta_0 = 70^\circ$ and the other physical parameters are, respectively, $m = 0.013m_e$, $g = 51$, $d = 50$ nm, $B = 0.5$ T, and $n = 5$. Solid (red) and dashed (blue) lines correspond to spin-up and spin-down polarized electrons.

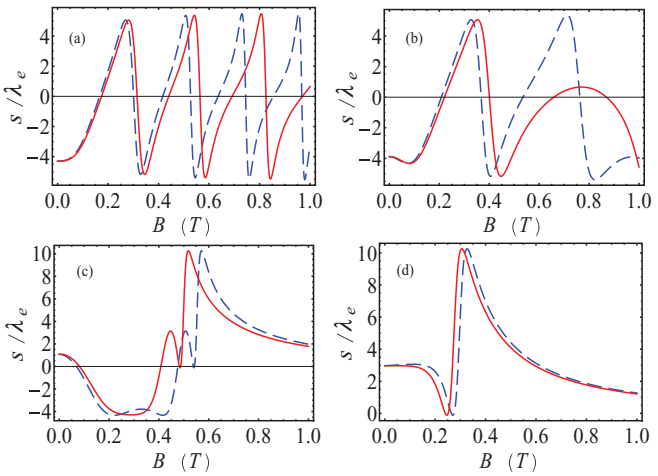

FIG. 3. (Color online) Dependence of the Goos-Hänchen shift on the strength of magnetic field B with different Landau quantum numbers $n = 0$ (a), $n = 1$ (b), $n = 3$ (c), $n = 5$ (d), where $\theta_0 = 70^\circ$, $E = 17.81$ meV, and the other physical parameters are the same as those in Fig. 2. Solid (red) and dashed (blue) lines correspond to spin-up and spin-down polarized electrons.

for transmission resonances with changing magnetic fields. In other words, in the propagating case, the Goos-Hänchen shifts can be changed from negative to positive by controlling the strength of the magnetic field, and vice versa. However, the Goos-Hänchen shifts finally become positive with increasing the strength of the magnetic field, due to the fact that the critical energy becomes larger than the incident energy with a enough large magnetic field B_c, and the propagation of electrons is actually evanescent in this case. To better understand the dependence of shifts on the magnetic field, we have to calculate the critical magnetic field B_c from Eq. (17) by solving the following equation, $(n+1/2)\hbar e^2 B_c^2/m^2 + \mu_B g\sigma B_c/2 + (n+1/2)\hbar\omega_0^2 - E = 0$, for the fixed incident energy E. For example, the critical magnetic fields for spin-up and spin-down polarized electrons can be numerically obtained as follows: $B_c^+ = 1.02$ T and $B_c^- = 1.48$ T for $n = 1$, $B_c^+ = 0.49$ T and $B_c^- = 0.55$ T for $n = 3$, and $B_c^+ = 0.28$ T and $B_c^- = 0.30$ T for $n = 5$. So these results can be applicable to explain the most striking effect around the critical magnetic field B_c in Figs. 3(b)–3(d), while a similar behavior is not shown in Fig. 3(a), because the critical magnetic fields, $B_c^+ = 3.00$ T and $B_c^- = 5.98$ T for $n = 0$, are too large, and we just show the range of magnetic field from 0 to 1 T due to the physical restriction to applied magnetic field in the laboratory. In addition, another observation from Fig. 3 is that, with increasing Landau quantum number n, the curves of the Goos-Hänchen shifts move leftward. That is to say, for the given incident energy, the Landau energy level leads to the fact that the resonant peak or the critical strength of magnetic field B_c shifts toward the low magnetic field strength region with increasing Landau quantum number n. Compared to the previous results in the magnetic-electric nanostructure,[9] the magnetic field and Landau quantum number provide more freedom to control the quantum Goos-Hänchen shift for ballistic electrons, which is useful to their application in semiconductor devices.

Now, we will discuss the spin beam splitting by the spin-dependent Goos-Hänchen shifts at various incidence angles. In general, the Goos-Hänchen shifts can be modulated also by the incidence angles, due to the energy dispersion (8). In Fig. 4(a), we would like to emphasize that the spin-up and spin-down polarized electrons can be spatially separated by the spin-dependent Goos-Hänchen shifts at large incidence angles, for example, $\theta_0 = 80°$, where incident energy $E/E_0 = 7.8$, and the other physical parameters are the same as those in Fig. 2.

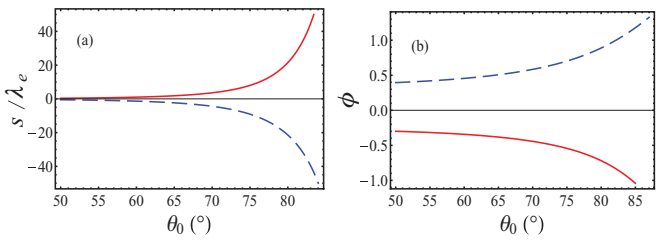

FIG. 4. (Color online) Spin-dependent Goos-Hänchen shifts (a) and corresponding phase shifts (b) as the function of incidence angle, where $E/E_0 = 7.8$ and the other physical parameters are the same as those in Fig. 2. Solid (red) and dashed (blue) lines represent spin-up and spin-down polarized electrons, respectively.

To confirm this intriguing result, the phase shifts of transmitted electrons have been investigated also in Fig. 4(b). In detail, the negative slope of the phase shift with respect to the incidence angle will result in a positive Goos-Hänchen shift, whereas the positive slope will lead to a negative Goos-Hänchen shift, which is in agreement with theoretical predictions made by the stationary phase method. Thus, the Goos-Hänchen shifts can be explained by the reshaping process of the transmitted beam, since each plane-wave component undergoes a different phase shift due to multiple reflections inside the quantum well.[18] The negative and positive beam shifts are usually considered as consequences of constructive and destructive interferences between the plane-wave components of the electron beam.

B. Numerical simulation

In this section, we proceed further to make numerical simulations of the incident Gaussian-shaped beam, $\Psi_{\text{in}}(x = 0, y) = \exp(-y^2/2w_y^2 + ik_{y0}y)$, where $w_y = w\sec\theta_0$, and w is the width of the beam. According to the Fourier integral, using Eqs. (11) and (12), we can obtain the wave function of the transmitted beam as follows,

$$\Psi_{tr}(x,y) = \frac{1}{\sqrt{2\pi}}\int_{-k}^{k} DA(k_y - k_{y0})e^{i[k_x(x-d)+k_y y)]}\,dk_y, \quad (21)$$

where $A(k_y - k_{y0}) = w_y \exp[-(w_y^2/2)(k_y - k_{y0})^2]$. For a well-collimated beam the range of the above integral can be ideally extended from $-\infty$ to ∞. Figures 5(a) and 5(b) illustrate the distribution of the transmitted beam, $|\Psi_{\text{tr}}(x,y)|^2$, for spin-up and spin-down polarized electrons, where $\theta_0 = 80°$, the beam width is $w = 5\lambda_e$, and the other physical parameters are the same as those in Fig. 2. As demonstrated

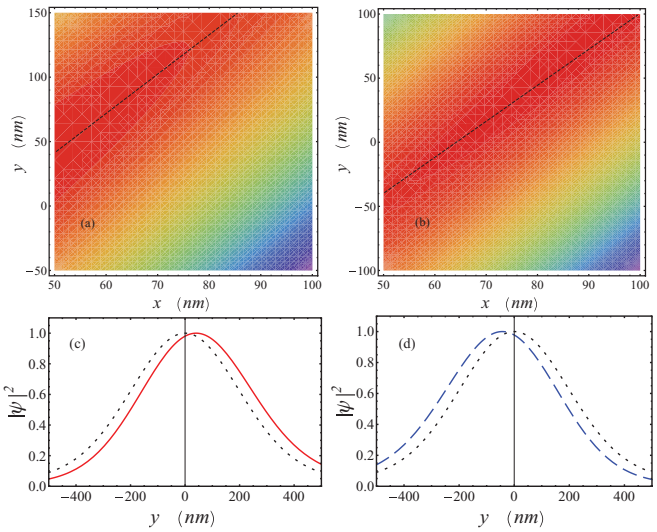

FIG. 5. (Color online) Distribution of the transmitted Gaussian-shaped beam for spin-up (a) and spin-down (b) polarized electrons, where $\theta_0 = 80°$, the beam width is $w = 5\lambda_e$, and the other physical parameters are the same as those in Fig. 2. Dashed lines represent the loci of maximum values for the eye. Profiles of the normalized incident and transmitted beams for spin-up (c) and spin-down (d) polarized electrons are also compared at $x = d$, where solid (red) and dashed (blue) lines represent the transmitted beams, and the dotted (black) line represents the incident beam as reference.

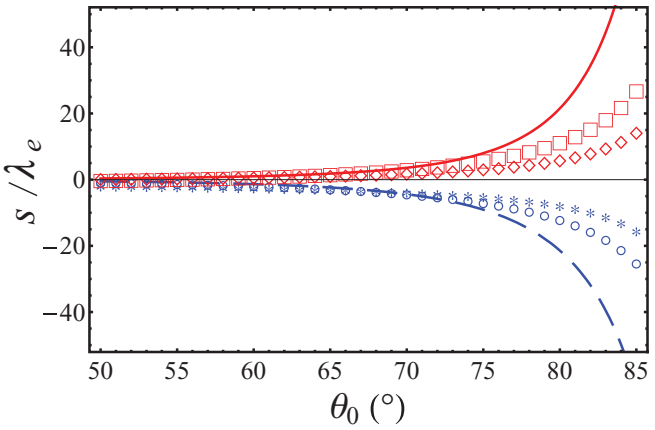

FIG. 6. (Color online) Influence of beam width on the Goos-Hänchen shifts, where the physical parameters are the same as those in Fig. 4. Solid (red) and dashed (blue) lines represent the shifts for spin-up and spin-down polarized electrons, calculated by stationary phase method. Lines with symbols □ (○) and ◇ (∗) correspond to the numerical results for spin-up (spin-down) polarization with $w = 10\lambda_e$ and $w = 5\lambda_e$, respectively.

in Figs. 5(a) and 5(b), dashed lines represent the loci of the maximum values for distribution of the transmitted beams for the eye. Evidently, the comparison between the normalized incident and transmitted beams at $x = d$ in Figs. 5(c) and 5(d) show that the positive and negative lateral shifts correspond to different spin polarizations. To find the numerical value of the beam shifts, we can find that position y corresponds to a maximum value of $|\Psi_{\rm tr}(x, y)|^2$. For the given parameters in Fig. 5, $y^+ = 40.80$ nm and $y^- = -43.21$ nm can be achieved for spin-up and spin-down polarized electrons, which are large enough to separate the different spin-polarized electrons beam spatially.

In Fig. 6, the numerical results further show the influence of beam width on the Goos-Hänchen shifts and spin beam splitter, where the physical parameters are the same as those in Fig. 4, and the beam width is chosen to be $w = 5\lambda_e$ and $w = 10\lambda_e$ (corresponding to beam divergences of $\delta\theta = 4^\circ$ and $\delta\theta = 2^\circ$). It is demonstrated that the wider the local waist is of the incident beam, the closer the numerical results are to the theoretical results predicted by the stationary phase method. It is worthwhile to point out that there is a discrepancy between the theoretical results predicted by the stationary phase approximation and the numerical results, resulting from the distortion of the transmitted electron beam,[9,18] especially when the local beam waist is narrow, which implies a large beam divergent $\delta\theta = \lambda_e/(\pi w)$. Actually, the stationary phase approximation is valid only for a well-collimated electron beam.[9,18] In detail, when the incidence angle is small enough, the Goos-Hänchen shifts predicted by the stationary phase method are in agreement with the results given by numerical simulations. But when a large incidence angle is chosen, $\delta\theta \ll 90^\circ - \theta_0$ is not satisfied, so that the transmitted beam shape will undergo a severe distortion. It is suggested that one cannot achieve an arbitrarily large Goos-Hänchen shift in practice by increasing the incidence angle, taking into account the influence of the finite beam width. In a word, the theoretical results of the stationary phase method and numerical simulations show that the simultaneously large and opposite beam shifts for spin-up and spin-down polarized electrons allow this system to realize the spin beam splitter, which can completely separate the spin-up and spin-down polarized electrons in such a semiconductor quantum device.

IV. DISCUSSION AND CONCLUSION

We have investigated the Goos-Hänchen shift for ballistic electrons through a parabolic quantum well under a uniform magnetic field. Due to the effect of the magnetic field, the Goos-Hänchen shift for ballistic electrons also becomes spin dependent, which leads to the unique applications in designing the spin filter and spin beam splitter. It is found that the Goos-Hänchen shift can be modulated by the incident energy, magnetic field, Landau quantum number, and incidence angle. In addition, we would like to mention that the Goos-Hänchen shift is also sensitive to the device geometry, since the lateral shift depends periodically on the width d of the parabolic quantum well region. The spin-dependent Goos-Hänchen shift and spin beam splitter presented here can be discussed in GaAs/AlGaAs-based quantum well structures,[23] rather than InSb semiconductors with a high g factor.

Last but not least, the Goos-Hänchen shift and relevant transverse Imbert-Fedorov effect in such a quantum well under the magnetic field may have a close relation to the spin Hall effect,[17,27,28] which deserves further investigation. We hope all the results presented here will stimulate further theoretical and experimental research on quantum Goos-Hänchen shifts for ballistic electrons in semiconductors[9,19] and graphene[12,29] and their applications in various quantum electronic devices.

ACKNOWLEDGMENTS

X.C. thanks Y. Ban and Z.-F. Zhang for helpful discussions. This work was supported by the National Natural Science Foundation of China (Grants No. 60806041 and No. 60877055) and the Shanghai Leading Academic Discipline Program (Grant No. S30105). X.C. also acknowledges funding by Juan de la Cierva Programme, Basque Government (Grant No. IT472-10) and Ministerio de Ciencia e Innovación (FIS2009-12773-C02-01).

*Author to whom correspondence should be addressed: xchen@shu.edu.cn

[1] H. K. V. Lotsch, Optik (Stuttgart) **32**, 116 (1970); **32**, 189 (1970); **32**, 299 (1971); **32**, 553 (1971).
[2] F. Goos and H. Hänchen, Ann. Phys. **1**, 333 (1947); **5**, 251 (1949).
[3] K. V. Artmann, Ann. Phys. **437**, 87 (1948).
[4] R.-H. Renard, J. Opt. Soc. Am. **54**, 1190 (1964).
[5] J. L. Carter and H. Hora, J. Opt. Soc. Am. **61**, 1640 (1971).

[6]R. Briers, O. Leroy, and G. Shkerdinb, J. Acoust. Soc. Am. **108**, 1624 (2000).
[7]V. K. Ignatovich, Phys. Lett. A **322**, 36 (2004).
[8]V.-O. de Haan, J. Plomp, T. M. Rekveldt, W. H. Kraan, A. A. van Well, R. M. Dalgliesh, and S. Langridge, Phys. Rev. Lett. **104**, 010401 (2010).
[9]X. Chen, C.-F. Li, and Y. Ban, Phys. Rev. B **77**, 073307 (2008).
[10]J.-H. Huang, Z.-L. Duan, H.-Y. Ling, and W.-P. Zhang, Phys. Rev. A **77**, 063608 (2008).
[11]L. Zhao and S. F. Yelin, Phys. Rev. B **81**, 115441 (2010); e-print arXiv:0804.2225v2.
[12]C. W. J. Beenakker, R. A. Sepkhanov, A. R. Akhmerov, and J. Tworzydło, Phys. Rev. Lett. **102**, 146804 (2009).
[13]M. Sharma and S. Ghosh, J. Phys. Condens. Matter **23**, 055501 (2011).
[14]S. C. Miller Jr. and N. Ashby, Phys. Rev. Lett. **29**, 740 (1972).
[15]D. M. Fradkin and R. J. Kashuba, Phys. Rev. D **9**, 2775 (1974); **10**, 1137 (1974).
[16]D. W. Wilson, E. N. Glytsis, and T. K. Gaylord, IEEE J. Quantum Electron. **29**, 1364 (1993).
[17]N. A. Sinitsyn, Q. Niu, J. Sinova, and K. Nomura, Phys. Rev. B **72**, 045346 (2005).
[18]X. Chen, C.-F. Li, and Y. Ban, Phys. Lett. A **354**, 161 (2006).
[19]X. Chen, Y. Ban, and C.-F. Li, J. Appl. Phys. **105**, 093710 (2009).
[20]V. M. Ramaglia, D. Bercioux, V. Cataudella, G. D. Filippis, and C. A. Perroni, J. Phys. Condens. Matter. **16**, 9143 (2004).
[21]X.-D. Zhang, Appl. Phys. Lett. **88**, 052114 (2006).
[22]M. Khodas, A. Shekhter, and A. M. Finkel'stein, Phys. Rev. Lett. **92**, 086602 (2004).
[23]F. Wan, M. B. A. Jalil, S. G. Tan, and T. Fujita, J. Appl. Phys. **103**, 07B731 (2008); Int. J. Nanoscience **8**, 71 (2009).
[24]S. Datta, *Electronic Transport in Mesoscopic Systems* (Cambridge University Press, Cambridge, U.K., 1995).
[25]D. Bohm, *Quantum Theory* (Prentice-Hall, New York, 1951), p. 259.
[26]M. Büttiker, Phys. Rev. Lett. **57**, 1761 (1986).
[27]M. Onoda, S. Murakami, and N. Nagaosa, Phys. Rev. Lett. **93**, 083901 (2004).
[28]K. Yu. Bliokh and V. D. Freilikher, Phys. Rev. B **74**, 174302 (2006).
[29]Z.-H. Wu, F. Zhai, F. M. Peeters, H. Q. Xu, and K. Chang, Phys. Rev. Lett. **106**, 176802 (2011).